Biol. Cybern. 66, 217–230 (1992)

Biological Cybernetics

© Springer-Verlag 1992

A model for the coordinated development of columnar systems in primate striate cortex

N. V. Swindale

Department of Ophthalmology, University of British Columbia, 2550 Willow Street, Vancouver, BC, Canada V5Z 3N9

Received January 21, 1991/Accepted in revised form May 28, 1991

Abstract. The existence of patchy regions in primate striate cortex in which orientation selectivity is reduced, and which lie in the centers of ocular dominance stripes is well established (Hubel and Livingstone 1981). Analysis of functional maps obtained with voltage sensitive dyes (Blasdel and Salama 1986) has suggested that regions where the spatial rate of change of orientation preference is high, tend to be aligned either along the centers of ocular dominance stripes, or to intersect stripe borders at right angles. In this paper I present results from a developmental model which show that a tendency for orientation selectivity to develop more slowly in the centers of ocular dominance stripes would lead to the observed relationships between the layout of ocular dominance and the map of orientation gradient. This occurs despite the fact that there is no direct connection between the measures of preferred orientation (from which the gradient map is derived) and orientation selectivity (which is independent of preferred orientation). I also show that in both the monkey and the model, orientation singularities have an irregular distribution, but tend to be concentrated in the centers of the ocular dominance stripes. The average density of singularities is about $3/\lambda_\theta^2$, where λ_θ is the period of the orientation columns. The results are based on an elaboration of previous models (Swindale 1980, 1982) which show how, given initially disordered starting conditions, lateral interactions that are short-range excitatory and long-range inhibitory can lead to the development of patterns of orientation or ocular dominance that resemble those found in monkey striate cortex. To explain the coordinated development of the two kinds of column, it is proposed that there is an additional tendency in development for the rate of increase in orientation selectivity to be reduced in the centers of emerging ocular dominance stripes. This might come about if a single factor modulates plasticity in each cell, or column of cells. Thus plasticity may be turned off first in regions in the centers of ocular dominance stripes where relatively extreme and therefore stable ocular dominance values are achieved early in development. Consequently it will be hard for cells in these columns to modify other properties such as orientation preference or selectivity.

1 Introduction

Neurons in the striate cortex of primates have responses to visual stimuli that can be characterised in several different ways. Most neurons will respond when a light or dark bar is moved across a particular region in visual space, but the response is usually dependent on the orientation of the bar or edge, with one particular orientation causing a larger response than others (Hubel and Wiesel 1968). Neighbouring cells tend to have similar orientation preferences, as do cells located in columns that run from pia to white matter in a direction perpendicular to the cortical surface (Hubel and Wiesel 1968).

Most neurons respond to a stimulus whether it is seen through the right or the left eye, but the two eyes are usually not equally effective in evoking a response. Cells can therefore be characterised in terms of the relative strengths of the inputs from each eye, a property known as ocular dominance. A complete range of ocular dominance values is found in the cortex, with some cells sensitive only to the left eye, others that are nearly equally sensitive to both eyes, and others that respond only to stimuli presented to the right eye (Hubel and Wiesel 1968). As with orientation preference, cells in the same column of tissue tend to have the same ocular dominance.

These two parameters, preferred orientation and ocular dominance, although constant with depth, change systematically with lateral (or tangential) distance in the striate cortex. A graph of ocular dominance against distance in a direction tangential to the cortical surface, shows a roughly sinusoidal variation, with a period of slightly less than a millimeter. A similar graph of preferred orientation shows nearly linear rates of change of orientation with distance, interrupted by occasional reversals in the direction of change, as well

as sudden jumps in preferred orientation, with a single 180° rotation occurring on average every 600 μm (Hubel and Wiesel 1968, 1974a).

An anatomical basis for the variations in ocular dominance was first demonstrated by Hubel and Wiesel (1972) who showed that the visual pathways from the left and right eyes to the cortex are segregated within layer IV of the cortex, into a pattern of stripes innervated alternately by the left and right eyes. This can be demonstrated most clearly by injecting a radio-active tracer into one eye and then examining the resulting distribution of radioactivity in sections cut tangential to the surface of the striate cortex (Wiesel et al. 1974). This shows that each eye's inputs form a pattern of branching stripes, the patterns for right and left eyes being complementary, with a periodicity of about 800 μm. The distribution of inputs revealed anatomically, predicts the variations in ocular dominance measured physiologically (LeVay et al. 1975; Hubel et al. 1977).

No structural correlates of orientation selectivity have yet been demonstrated in striate cortex, and it has proved difficult to determine the nature of the two-dimensional layout. However, recent work using voltage sensitive dyes (Blasdel and Salama 1986) has shown that iso-orientation domains (regions within which orientation preference lies between some defined range) are short elongated strips of variable width, with no consistent overall direction of elongation (Fig. 1a). The maps of orientation preference revealed by this technique are also characterised by points where single complete sets of orientation domains meet, known as singularities.

The possibility of a structural relationship between orientation and ocular dominance columns was first suggested by Horton and Hubel (1981) and Hubel and Livingstone (1981). Although the interpretation of Horton and Hubel's results was problematic, a possible conclusion that could be drawn from their data was that different iso-orientation domains meet, forming singularities, in regions of poor orientation selectivity. Hubel and Livingstone's data showed that regions of poor orientation selectivity did indeed exist in the upper layers of the striate cortex, and that these regions coincided with patches of high cytochrome oxidase activity. Horton and Hubel (1981) and Hendrickson et al. (1981) then showed that the cytochrome patches coincided with the centers of individual ocular dominance stripes leading to the suggestion (Swindale 1981) that the orientation singularities might be located close to the cytochrome patches in the centers of ocular dominance stripes.

Blasdel and Salama (1986) provided evidence for a somewhat different kind of structural relationship between the layout of orientation preference, and the ocular dominance stripes. By applying a spatial gradient operator to the map of orientation preference they showed that regions of high orientation gradient (termed 'fractures') were short strips aligned in a direction either parallel to the direction of the ocular dominance stripes, or orthogonal to them (Fig. 1b) and also closely associated with the cytochrome patches (Fig. 1d). Although the singularities lie within these regions of high orientation gradient, the association between the singularities and the centers of the ocular dominance stripes is much less obvious (Fig. 2).

Two related models were devised to account for the formation of ocular dominance stripes (Swindale 1980) and for the pattern of iso-orientation domains (Swindale 1982). The models described how each set of columns might develop in time, given nearly uniform starting conditions. Inputs from the left and right eyes in the cortex were assumed to be intermingled initially, with only randomly occurring fluctuations in the density (Rakic 1977). Likewise, orientation preferences were assumed to be slight, and randomly distributed among neurons. Following this, growth, either of the number of left or right eye synapses, or of orientation selectivity, was assumed to occur subject to the condition that points close together (e.g. less than 250 μm) would tend to have similar orientation or ocular dominance values, while points an intermediate distance apart (e.g. 250–600 μm) would tend to have opposing ocular dominance values, or orthogonal orientation preferences. The model for ocular dominance stripes produced patterns that were similar to those observed in both cat and monkey, while the model for iso-orientation domains (in the 180° form: Swindale 1982) predicted an arrangement like that subsequently found in both cat (Swindale et al. 1987; Bonhoeffer and Grinvald 1990) and macaque monkey (Blasdel and Salama 1986).

Given the success of the two models, it is natural to ask if there is some way of linking them so as to produce the kinds of structural correspondence between the maps of orientation preference and of ocular dominance that are observed experimentally. The purpose of this paper is to show that it is enough to assume that the rate of increase in orientation selectivity in development is slowed in regions near the centers of the emerging ocular dominance stripes. This leads to structural relations between the orientation and ocular dominance patterns that are similar to those found in the monkey, with orientation singularities tending to be located in the centers of the ocular dominance stripes, and strip-like regions of high orientation gradient which run either parallel, or orthogonal to, the borders of ocular dominance columns.

2 The experimental data

By using a voltage sensitive dye, Blasdel and Salama (1986) were able to record the distribution of electrical activity evoked by various kinds of visual stimuli over a large (5 × 8 mm approx) area of striate cortex in the macaque monkey. They were able to demonstrate for the first time, the two-dimensional layout of orientation preference in the cortex (Fig. 1a) and a spatial derivative of this (the orientation gradient: Fig. 1b). In the same tissue they demonstrated the distribution of ocular dominance (Fig. 1c), the distribution of the magnitude of the orientation selectivity (not shown), and by subsequent histology, the distribution of cytochrome

oxidase activity (Fig. 1d). In order to facilitate comparison of these data with the patterns generated by computer simulation, a detailed description of the experimental results will be given here, together with the results of some further graphical analysis of the data reproduced in Fig. 1.

2.1 Orientation preference

The map of orientation preference was presented as a colour coded map, with neighbouring colours in the spectrum (red, orange, yellow, green, blue, purple) representing neighbouring orientations. The pattern is visually complex, but a number of general features are clearly evident.

Individual iso-orientation domains (regions with the same colour in Fig. 1a) are variable in shape, but are often curved and scalloped with a half-moon shape being relatively common. Locally, sets of domains often form parallel bands, but these rarely extend more than a millimeter, and the direction of the bands varies from region to region.

The patterns shown in Fig. 1a and c are obviously periodic although Blasdel and Salama did not state what the periodicities were, nor was a scale bar given. However since Figs. 1a and c are of identical areas of cortex at the same scale it is possible to estimate the ratio between orientation and ocular dominance periodicities. I did this by measuring the distances between the centers of 24 pairs of similarly coloured regions in Fig. 1a, the members of each pair being separated by a single 180° cycle of orientations. The same thing was done for Fig. 1c, taking distances between the centers of neighbouring ocular dominance stripes (12 pairs). The ratio between the average of each set of measurements was 0.76 (ori/od), which is similar to previous estimates (Hubel et al. 1978).

Singularities, points where the sharp extensions of a single complete set of domains meet, are common. Their distribution (Fig. 2) is irregular; quite large areas lacking singularities occur, while two singularities often occur close together. Measurements were made of the overall density of singularities in Fig. 2, omitting regions (predominantly on the left of the figure) where the pattern of ocular dominance seemed obscure. The overall density of singularities was $3.03/\lambda_\theta^2$, where λ_θ is the orientation column period. This is similar to the density in area 18 of the cat (Swindale et al. 1987) which is $2.7/\lambda_\theta^2$ ($\lambda_\theta = 1.23$ mm in cat area 18).

In order to discover whether or not the singularities shown in Fig. 2 tend to be located in the centers of ocular dominance stripes, the picture was digitised and the area within which singularities were counted was then divided into two complementary and nearly equal areas. The first area, occupying 48% of the total, included all regions within a given distance (about 100 μm) of the border of an ocular dominance stripe, and the second, occupying 52% of the total area, included all other regions i.e. those in the centers of the stripes. The number of singularities counted in the central regions of the stripes (69) was greater than the number occurring close to the edges (42), and (taking into account the slight difference in areas) this association was statistically significant ($p \approx 0.022$).

2.2 Orientation gradient

The map of orientation gradient is also periodic, with regions of high gradient, termed 'fractures' by Blasdel and Salama, forming an irregularly branched series of ridges enclosing or partly enclosing patchy regions of low gradient. Not surprisingly, the orientation singularities all lie within regions of high gradient, although regions of high gradient do not always contain singularities. Blasdel and Salama noted a tendency for these gradient strips to run either parallel to ocular dominance stripes, or orthogonal to them (Fig. 1c) although not all strips conform to this rule and intersections at other angles are quite common. There is also an association between regions of high orientation gradient and cytochrome oxidase patches, which are known to lie in the centers of ocular dominance stripes (Fig. 1d): the strips run adjacent to, or in the centers of, the patches, and often join neighbouring patches.

3 The model

The following is a brief description of the models of ocular dominance and orientation column development put forward earlier (Swindale 1980, 1982).

3.1 Ocular dominance

The scalar variable n will be used to represent the value of ocular dominance at position $r = (x, y)$ on the cortical surface. It is convenient to let ocular dominance values be represented on a scale from -1 to $+1$, with -1 representing complete contralateral eye dominance and $+1$ representing complete ipsilateral dominance. The values of n are assumed to be initially normally distributed around a mean of zero (corresponding to equal inputs from both eye, or ocular dominance group 4) and with a standard deviation σ_n. At each position, n grows at a rate dependent on the surrounding values of n: the rate of growth is calculated by making a weighted sum of the surrounding values, the weights varying with distance, being positive for short distances, negative for intermediate ones, and tending to zero with increasing distance. If $w_n(r)$ is the function that describes how the weights change with distance, the rate of growth dn/dt is given by

$$\partial n/\partial t = n * w_n f(n)$$

where $*$ denotes convolution, and $f(n)$ is used to set a limit to the upper and lower values of n: its value should be positive for all values of $-1 < n < +1$ and tend to zero as n approaches values of -1 or $+1$. A

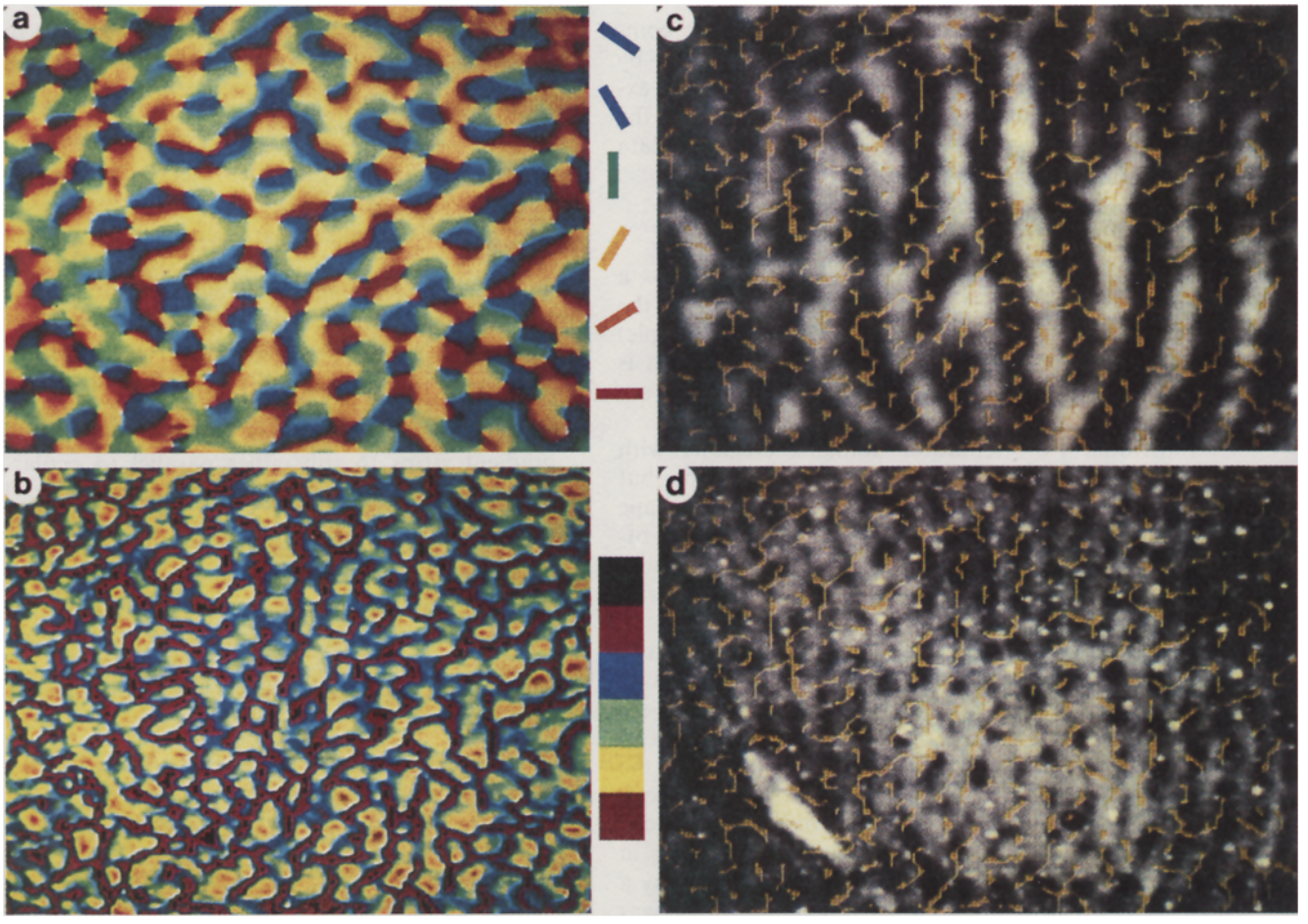

Fig. 1

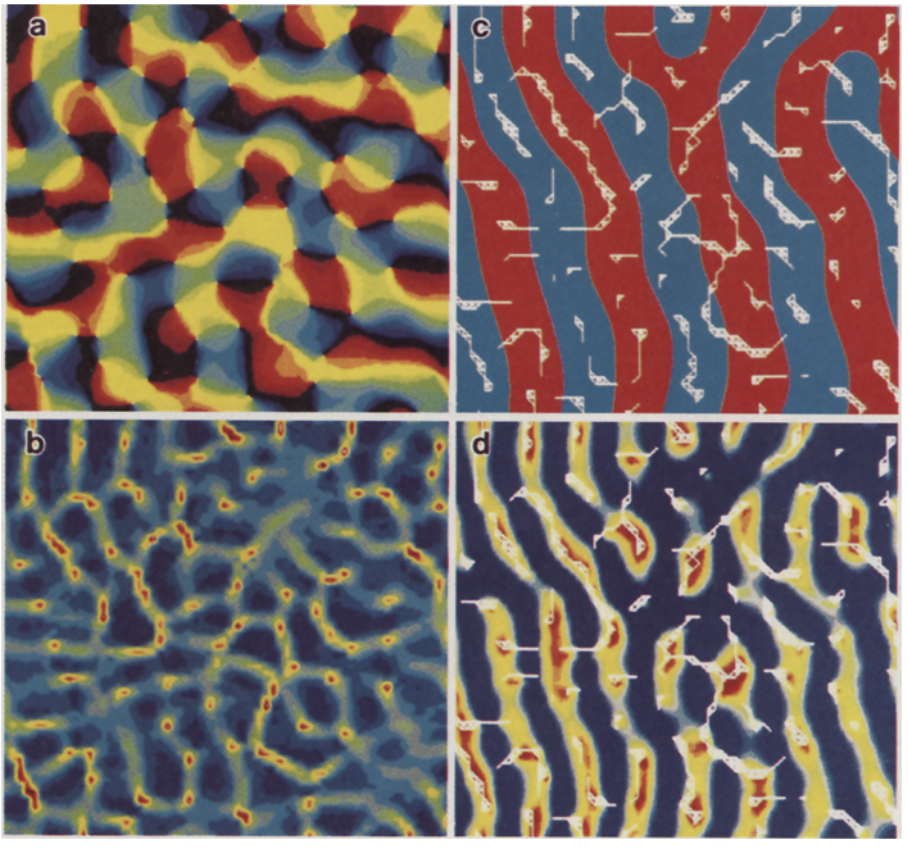

Fig. 4

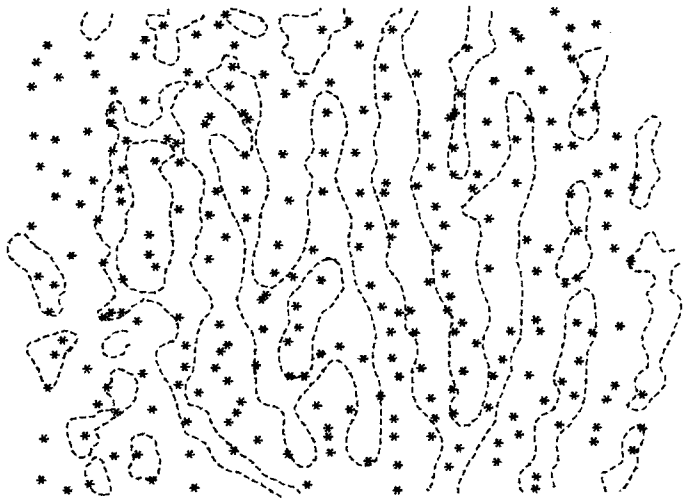

Fig. 2. The distribution of orientation singularities (*asterisks*) obtained by visual inspection of Fig. 1a, and superimposed on the pattern of ocular dominance stripes redrawn from Fig. 1c. Boundaries between stripes are shown as dashed lines. Note the occurrence of relatively large areas free of singularities, as well as the occurrence of pairs that are close together, and that singularities are often located on the borders between stripes, as well as in their centers

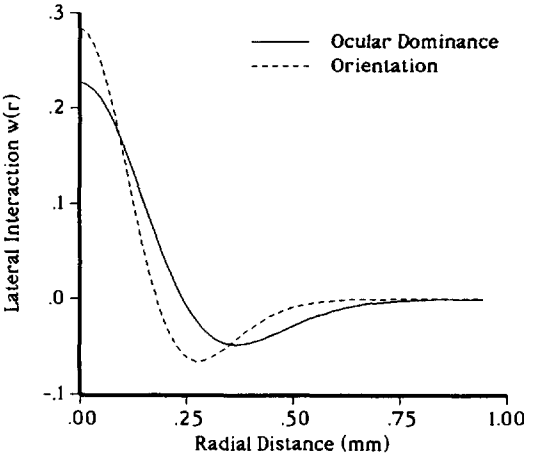

Fig. 3. The two lateral interaction functions, w_n and w_z, used to generate the pattern shown in Fig. 4. Assuming ocular dominance has a period of 800 μm, 20 array units ≈1 mm in the cortex. Parameter values for w_n (3.2) were $A = 0.541$; $B = 0.314$; $d_1 = 21.87$; $d_2 = 44.73$ and $\beta = 1.3$ (the value of w_n along the x axis is graphed here); corresponding values for w_z were $A = 0.717$; $B = 0.433$; $d_1 = 12.86$; $d_2 = 25.72$ and $\beta = 1.0$. These values were calculated to give periodicities for ocular dominance and orientation = 800 μm and 600 μm (16 and 12 array units) respectively

simple function that has this property is $f(n) = (1 - n^2)$, thus giving a complete equation for the growth of ocular dominance:

$$\partial n/\partial t = n * w_n(1 - n^2) \tag{3.1}$$

where

$$|n * w| < 1 .$$

It is convenient to let w_n be a difference of Gaussians,

$$w_n(x, y) = A \exp\{-(\beta x^2 + y^2)/d_1\} - B \exp(-(x^2 + y^2)/d_2\} \tag{3.2}$$

with A, B, d_1, d_2 positive constants; $A > B$, $d_2 > d_1$, and x and y position coordinates. The constant β allows the central positive region of w_n to be elongated in either the x or y direction, depending on whether β is greater or less than 1. This has the effect of causing the stripes that form to take on a consistent direction of elongation. Other functions, which are similarly positive for small values of r, negative for an intermediate range of distances, and zero elsewhere, can also be used with similar results.

3.2 Orientation

The equation that describes the development of orientation columns is analogous to the one for ocular dominance, with the difference that the quantity representing orientation is a complex number $z = a + ib$. For reasons discussed elsewhere (Swindale 1982, Swindale et al. 1987), it is supposed that the orientation represented by z is:

$$\theta = \tfrac{1}{2} \arctan(b/a) \tag{3.3}$$

while the modulus of z, $|z| = (a^2 + b^2)^{1/2}$ is assumed proportional to some measure of the degree of orientation selectivity, selectivity being absent when $|z| = 0$, and maximal when $|z| = 1$. The same vector measure of orientation is used for the statistical analysis of orientation data (Batschelet 1981) while a similar connection between vector magnitude and orientation selectivity was also made by Blasdel and Salama. By analogy with

Fig. 1a–d. From Blasdel and Salama (1986): maps of **a** orientation preference, **b** orientation gradient, **c** ocular dominance and **d** cytochrome oxidase staining in monkey striate cortex. 'Fractures' – regions of exceptionally high orientation gradient are indicated by fine yellow lines in panels **c** and **d**. All four panels are from the same area of cortex and can thus be superimposed. Black regions in panel **b** indicate regions of gradient 45°/40 μm or greater. See text for further description

Fig. 4a–d. Results of the computer model: **a** the map of orientation preference, **b** orientation gradient, **c** ocular dominance and **d** orientation selectivity. As in Fig. 1, regions of high orientation gradient are indicated by fine white lines in panels **c** and **d**. In panel **b** regions of low orientation gradient are shaded blue and regions of high gradient are yellow or red; in panel **d** regions of high orientation selectivity are blue, and regions of low selectivity yellow and red. For this simulation, the coupling coefficient $a = 20$ (3.5), and values for w_n and w_z (Fig. 3) were calculated to give periodicities for ocular dominance and orientation of 16 and 12 array units respectively. Assuming a scaling of 20 array units = 1 mm of cortex, the gradient threshold for display of lines in panels **c** and **d** is equivalent to 35° in 40 μm. The display shows the state of the model after ≈600 program steps

the model for ocular dominance, values of z are assumed to be small and randomly distributed initially, and, in the original model, to change at rates given by

$$\partial z/\partial t = z * w_z(1 - |z|) \tag{3.4}$$

where w_z is defined as in (3.2) (although not necessarily with the same values of A, B, d_1 and d_2) and the term $1 - |z|$ ensures that $|z|$ has an upper limit of 1. As in (3.1), w is defined such that $|z * w| < 1$, which ensures that $|z| \leqslant 1$.

It is straightforward to obtain solutions to (3.1) and (3.4) by means of computer simulation: (3.1) produces patterns of branching stripes that resemble those observed in the monkey, while (3.4) produces a distribution of preferred orientation with irregularly spaced 180° singularities similar to that seen in both monkey and cat. The parameters A, B, d_1 and d_2 (3.2) which determine the shape of the lateral interaction function w, have the effect of determining the overall periodicity of the patterns that are formed, as well as the overall rate of growth (see (3.6a) and (3.6b) below). The actual details of the structures that form are consequences of the initial random (or unstructured) distribution of the values of n or z.

3.3 The link between orientation and ocular dominance

The fact that regions of poor orientation selectivity occur in the centers of ocular dominance columns implies that, during development, the rate of increase in orientation selectivity is retarded in the centers of the presumptive ocular dominance stripes i.e. in regions where ocular dominance is growing most rapidly. This coupling was modelled by writing

$$\partial z/\partial t = z * w_z(1 - |n * w_n|)^a(1 - |z|) \tag{3.5}$$

where a is a positive constant that describes the degree of coupling between the two systems. The quantity $|n * w_n|$ was used in preference to either n, or $\partial n/\partial t$, because it is largest in the centers of ocular dominance stripes, or presumptive stripes, at all stages of development, and is zero at, or close to the boundaries between stripes. $|\partial n/\partial t|$ on the other hand, although largest in the centers of the stripes early in development, tends to zero in these regions as n approaches values of ± 1 in the centers of the stripes, and is then largest between the centers and the edges. $|n|$ is unsatisfactory because its value remains small only at the edges of the stripes, and is eventually uniform in magnitude over almost all of the pattern. Note that when $a = 0$ the term $(1 - |n * w_n|)^a = 1$ and there is no coupling; for sufficiently large values of a, $(1 - |n * w_n|)^a$ tends monotonically to zero as the value of $|n * w_n|$ increases, providing that $|n * w_n| < 1$.

Equations (3.1), (3.2), (3.3) and (3.5) define the system that will be discussed in what follows. It is possible that other formulations of the hypothesis embedded in (3.5) might work satisfactorily; it is also possible to make the coupling between the systems reciprocal, and limit the rate of growth of n in regions where the growth of z is largest; for the sake of simplicity this effect has been omitted since it turned out not to be necessary to explain the existing data.

3.4 The computer simulations

Equations (3.1) and (3.5) can be solved given initial values for n and z, two sets of 5 parameters that define w_n and w_z (3.2), and a value for the coupling coefficient a. n was assumed to be normally distributed around a mean of zero, with $\sigma_n = 0.05$. The components of z, a and b, were similarly assumed to be normally distributed around a mean of zero with $\sigma_a, \sigma_b = 0.05$. n and z were represented as values stored in two-dimensional arrays of 64×64 points each.

Parameters for the lateral interaction functions, w_n and w_z, were calculated so as to produce patterns with defined periodicities and growth rates. It was shown in Swindale (1980) that the predominant spatial frequency in the pattern, v_m, is given by the spatial frequency for which the Fourier transform of $w(r)$, $W(v)$ has a maximum. The overall rate of development of the pattern is proportional to the amplitude, $g = W(v_m)$, of this frequency. With w defined by (3.2) and $\beta = 1$ it is possible to show that the period $\lambda = 1/v_m$

$$\lambda = \pi[(d_2 - d_1)/2 \log_e\{(d_2/d_1)(B/A)^{1/2}\}]^{1/2} \tag{3.6a}$$

and that

$$g = A\pi d_1(Ad_1^2/Bd_2^2)^{d_1/(d_2 - d_1)}(1 - d_1/d_2)\,. \tag{3.6b}$$

Another constraint on w is the volume under the function, $\bar{w}$. It is shown in Swindale (1982) that the average value of n, or z will tend to a stable value of 0, provided that $\bar{w} < 0$. $\bar{w}$ is given by

$$\bar{w} = \pi(Ad_1 - Bd_2)\,. \tag{3.6c}$$

With the addition of a fourth constraint that

$$k = d_2/d_1 \tag{3.6d}$$

(3.6a)–(3.6d) can be solved for A, B, d_1 and d_2 to give desired values of λ, g, $\bar{w}$ and k. It is generally more convenient to think of the model's parameter space as being in $\{\lambda, g, \bar{w}, k\}$ rather than in $\{A, B, d_1, d_2\}$. $\bar{w}$ and k had the constant values -6 and 2 respectively in all the simulations reported here, although as discussed below, these parameter values are uncritical over a wide range; λ was typically in the range 6–24, while values of g between 5 and 10 gave solutions that approached stability in around 200–500 program iterations with step size $\partial t = 1$. Convolutions with w were done by first calculating the Fourier transforms of n, z, w_n and w_z, multiplying, and carrying out the inverse transform. This is quicker than doing the convolutions directly.

The computations explored the effect of changing the relative periodicities of ocular dominance and orientation columns, the relative rates of growth, and the value of a, the coupling coefficient. In addition, the effect of making the columns spatially anisotropic (i.e. causing the ocular dominance stripes, or the iso-

orientation domains to run in a single preferred direction) was studied. This was done by setting $\beta = 1.3$ (3.2).

Orientation gradient, grad(θ), was calculated as follows:

$$\text{grad}(\theta_{i,j}) = \{h(|\theta_{i+1,j} - \theta_{i,j}|_{180})^2 + h(|\theta_{i,j+1} - \theta_{i,j}|_{180})^2\}^{1/2} \quad (3.7)$$

where

$h(\theta) = \theta \qquad \theta \leqslant 90°$

$h(\theta) = 180° - \theta \quad \theta \geqslant 90°$.

Note that θ, and thus grad(θ), is independent of the measure of orientation selectivity $|z|$, and that the two can, in principle, vary independently.

4 Results

Figure 4 illustrates the result of a simulation that is intended to mimic the experimental data from the macaque monkey. For this simulation, ocular dominance stripes are elongated vertically ($\beta = 1.3$, Eq. 2), with a period = 16 array units, and orientation had a period = 12 units, giving a periodicity ratio = 0.75, similar to the ratio in the monkey ($\approx$600 μm : 800 μm). The gains, g_n and g_z (6b) had values 8 and 6 respectively, and $a = 20$. Figure 3 graphs the lateral interaction functions w_n and w_z that were used to generate the patterns. Figure 4c shows the pattern of ocular dominance stripes formed, with regions of high orientation gradient indicated (as in Fig. 1c) by narrow white lines. The threshold for displaying these lines was similar to that used by Blasdel and Salama (Fig. 1c,d) assuming a scaling of 12 array units ≡ 600 μm. As in the monkey, there is an apparent tendency for these to run either parallel to the ocular dominance stripes, or orthogonal to them. Figure 4a shows the pattern of orientation columns formed, while Fig. 4b and d show maps of orientation gradient and the orientation modulus respectively. The orientation gradient map is also similar to that found in the monkey, being quasi-cellular in structure with ridges of high gradient enclosing or partially enclosing regions of low gradient. Regions where $|z|$ is low, i.e. regions of poor orientation selectivity, are blob-like, located over the centers of ocular dominance stripes, and tend to be associated with the ridges of high orientation gradient as in the monkey (Fig. 1d).

The relation between the regions of high gradient and the ocular dominance stripes was measured quantitatively in five maps generated with the same parameter values used to obtain Fig. 4, but using different random number seeds. Other than the initial choice of parameters and seed values, no subsequent selection process operated in choosing maps for analysis (this is true of all the quantitative analyses presented here, and in the following paper). In each map I calculated the local orientations of a) the od column boundaries and b) the local orientations of the regions of high orientation gradient, e.g. as shown by the white lines in Fig. 4c. (These orientations should not be confused with the "physiological" orientation preferences of the same regions as shown e.g. in Fig. 4a). The map of ocular dominance column border orientation was interpolated, using the Fourier algorithm described by Swindale et al. (1987) to obtain an orientation value for each point in the map. These orientation values (for example in the centers of the stripes) approximated the values of the closest border orientations. A histogram was then compiled showing the differences between the local orientation of each fracture zone, and the orientation computed from the ocular dominance map at that location. If the zones of high gradient tend to run either parallel, or orthogonal to the borders of ocular dominance stripes, this histogram should be peaked at around 0° and 90°. If, instead, they run at random angles across the ocular dominance stripes, all intersection angles should occur with equal frequency. The results of this analysis (Fig. 6) showed a rather broad distribution of intersection angles with an excess of intersections in the 0°–20° and 70°–90° ranges.

4.1 Singularities

Singularities in the model maps were identified, as in the monkey data, by eye and their density expressed as the number per λ_θ^2, where λ_θ is the average spacing of the iso-orientation domains. For the parameter values similar to those used to obtain Fig. 4 ($\lambda_\theta = 11.33$, $a = 20$, $\bar{w} = 6$, $k = 2$) the density was $= 3.34/\lambda_\theta^2$ ($n = 475$), which is similar to that measured in the monkey ($3.03/\lambda_\theta^2$). Coupling (i.e. the value of a) had little effect on the density, which was $3.14/\lambda_\theta^2$ ($n = 602$) when $a = 0$. Singularity density was also unaffected by the value of $\bar{w}$ over the range $-24 \leqslant \bar{w} \leqslant +3$. The value of k_z (6d: the ratio between the spreads of the inhibitory and excitatory surrounds of w_z) had a slight effect on density: when $k_z = 1.1$ the density = 3.05 ($n = 867$), and when $k_z = 12$ the density = 3.55 ($n = 1011$). The density appeared to vary linearly with k_z over this range.

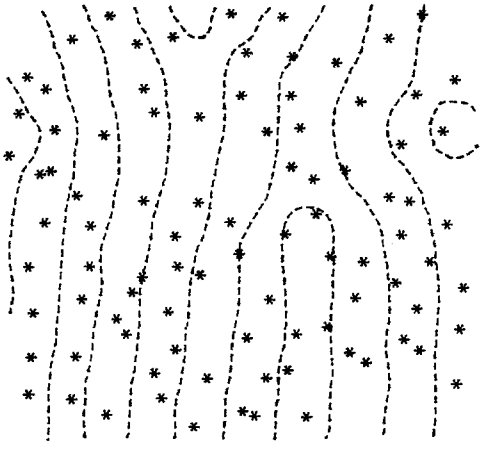

Fig. 5. The distribution of orientation singularities (*asterisks*) in a model pattern similar to the one shown in Fig. 4a, superimposed on the pattern of ocular dominance stripes (*dashed lines* indicate boundaries). Compare with the real data shown in Fig. 2

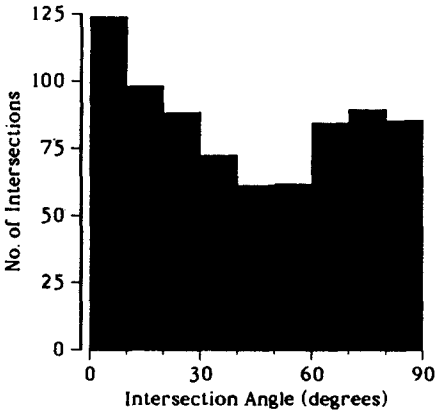

Fig. 6. The distribution of angles of intersection between regions of high orientation gradient ('fractures') and the orientations of nearby boundaries of ocular dominance stripes. A fracture zone running along the center of a stripe, parallel to the borders on either side, would yield intersection angles of zero along its length. Conversely, a straight fracture zone crossing a stripe at right angles would yield intersection angles of 90° along its entire length. Results were obtained from 5 different model maps, generated with the same parameters used to generate the map illustrated in Fig. 4

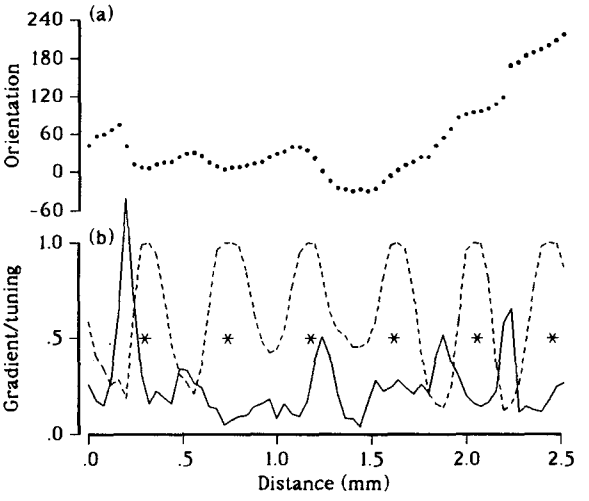

Fig. 7a,b. A simulated one-dimensional 'penetration' through a map similar to the one illustrated in Fig. 4. **a** shows orientation preference as a function of distance (in this case scaled so that 25 array units ≈ 1 cortical mm); **b** shows the corresponding values of orientation gradient (continuous line, vertical scaling is in units of approximately 1° per μm) and of orientation tuning (*dashed line*, a value of 1 indicates good tuning, and zero indicates no selectivity). Asterisks indicate points of transition i.e. the borders between ocular dominance columns

The positions of singularities in relation to the ocular dominance stripes was also measured, using the same method as described above for the monkey. Measurements were made on 5 different maps, obtained using the same parameters as those used to obtain Fig. 4. As for the monkey, the maps were divided into two complementary regions of nearly equal area, all regions (a) being within a given distance of a stripe boundary, and regions (b) elsewhere. This distance was chosen so that regions (a) and (b) occupied 49% and 51% of the total area respectively (the regions could not be exactly equal in area because of the discrete representation of positions used in computing the maps). About twice as many singularities were counted in region (b) ($n = 313/473$) as in region (a) ($n = 160/473$) and this difference is significant ($p < 0.0001$).

Figure 7 shows a sample one-dimensional 'electrode penetration' through a simulation similar to the one illustrated by Fig. 4. The graph shows how preferred orientation (dotted line), ocular dominance (asterisks), orientation selectivity (dashed line) and orientation gradient (continuous line) change with distance along a single 'electrode track' through the model. The asterisks mark boundaries between ocular dominance stripes. Note that orientation sequences can continue almost undisturbed through regions of poor orientation selectivity (e.g. in the second poor orientation patch from the right of Fig. 7), as was observed experimentally by Livingstone and Hubel (1984).

4.2 Stages in development

A number of stages in the development of the patterns shown in Fig. 4 are evident (Fig. 8):

1) There is an initial period (corresponding to a few weeks prenatal to just before birth in the monkey) when low amplitude periodic fluctuations in ocular dominance develop (Fig. 8d); the peaks and troughs of these fluctuations are strongly predictive of the centers of the stripes that will form later; at the same time, values of θ change sufficiently that considerable order is present in the orientation map (e.g. Fig. 8c,e); the orientation modulus $|z|$ however remains small (and by implication orientation selectivity is poor), and the orientation gradient map is also relatively disorderly (not illustrated).

2) In the following period (between the stages shown in Fig. 8e,f and 8g,h; probably corresponding to that between birth and 6 weeks of age in the monkey) ocular dominance stripes and iso-orientation domains become progressively better defined, $|z|$ begins to increase, most obviously at the edges of the ocular dominance stripes, while remaining small in the centers of the stripes. The orientation gradient map begins to show a well defined organization (c.f. Wiesel and Hubel 1974). At the end of this period, development of ocular dominance columns is essentially complete (Fig. 8h).

3) There follows a relatively long period (equivalent to months) during which $|z|$ continues to increase, while the patchy regions in the centers of the ocular dominance stripes in which $|z|$ is small slowly decrease in size. With time, these would disappear completely, with $|z| \to 1$ everywhere as $t \to \infty$, since the term $(1 - |n * w_n|)^a$ in (3.5) is always >0. This process can be slow however, especially if a is large, and might correspond to a period of up to a year in the monkey. It is likely that some other process, not modelled here, stabilises the values of orientation selectivity that are achieved at a variety of levels below the maximum possible. There is probably some laminar specificity in this process, since patchy regions of poor orientation selectivity are present only in the upper layers of the cortex.

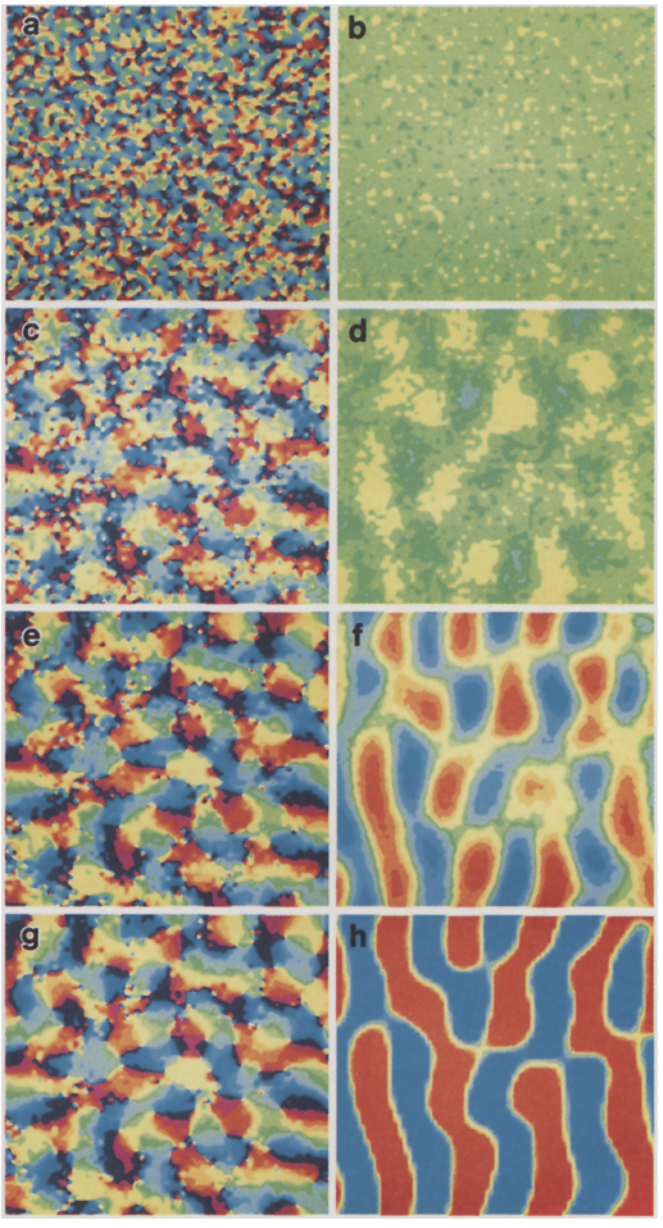

Fig. 8a–h. Stages in the development of a model cortex. Panels on the left (**a, c, e, g**) show orientation preference, and on the right, ocular dominance (**b, d, f, h**). Developmental times are $t = 1$; $t = 20$; $t = 40$ and $t = 80$ (program iterations). Panels **c, d** are representative of the state of cortex at around the time of birth, and panels **g, h** at around 6 weeks of age. Colour scales are (approximately) the same as in Fig. 4

The scatter plots in Fig. 9 show the relationships between orientation tuning (i.e. $|z|$), orientation gradient, and the smoothed ocular dominance measure $n * w_n$ for each point in a representative map. The latter measure was chosen in preference to n, since it depends on position within an ocular dominance stripe, being largest in the center and decreasing to zero at the edges. Figure 9a shows the relation between this measure of ocular dominance and $|z|$, and demonstrates the strong tendency for $|z|$ to be low in the centers of ocular dominance stripes, where $|n * w_n|$ is largest. This dependence is a simple consequence of the relationship between the two built in to (3.5). Figure 9b illustrates the weaker relationship between $|z|$ and grad(θ), but shows a clear tendency for grad(θ) to be large where $|z|$ is small. Figure 9c illustrates the tendency for grad(θ) to be large in the centers of the ocular dominance stripes. This can be considered to be an emergent property of the model, because grad(θ) is derived from orientation values which are obtained independently of the modulus of z. It is not straightforwardly dependent on the correlation between $|z|$ and $|n * w_n|$, because, as illustrated in Fig. 11 the correlation between grad(θ) and $|n * w_n|$ can vary independently of that between $|z|$ and $|n * w_n|$.

The model parameters that have the largest influence on the results just described are the coupling coefficient, a, the ratio between the growth rates g_z/g_n, the relative periodicities of the two sets of columns, and whether or not one or both sets of columns is elongated in a particular direction. The correlation between orientation gradient and ocular dominance, measured by calculating the product-moment correlation coefficient between the two variables, was found to be roughly linearly proportional to a, over a range of values of a from 0–30, and to g_z/g_n over a range of ratios 0.5 to 1.5. If g_z/g_n is small and a large however the rate of increase in $|z|$ becomes unrealistically slow, and singularity density is also high. Conversely, if a is small (e.g. <10) and g_z/g_n large (e.g. $=1.5$) then $|z|$ becomes large, and consequently stable, before ocular dominance stripes start to form, and the two systems remain largely independent.

Many of the other model parameters have only small effects on the results, and their choice of values seems to be arbitrary within a fairly large range. This is demonstrated in Fig. 10, which shows the effect, on three indices of the model's performance, of different values of the parameters k_z, k_n, $\bar{w}_z$, $\bar{w}_n$, σ_z and σ_n. Each of these parameters was assigned one of two values, thereby defining a 6-bit number, the order of bits being the same as the order of parameters just given. The value of this number is graphed on the horizontal axis of Fig. 10. The numbers comprising each pair of values differed in magnitude by a factor of four or more, and straddled the values used elsewhere in this, and the following paper. All 64 possible combinations of the pairs were tested. The indices of the model's performance that were measured were *a)* the density of singularities in the orientation map (asterisks); *b)* the correlation between $|z|$ and $|n * w^n|$ (filled circles) and *c)* the correlation between grad(θ) and $|n * w_n|$ (empty circles). Although not all of the various combinations of parameter values give ideal results, it is clear that there are many different combinations that give essentially similar results by these measures. Many of these effects (e.g. those due to change in σ_z and σ_n) could be attributed to changes in the rates of development of the orientation and ocular dominance patterns, with the effects mentioned above. There were no obvious effects of the values of $\bar{w}_z$, $\bar{w}_n$ or k_z over the ranges tested.

Figure 11 shows how coupling between orientation gradient and ocular dominance depends on the period-

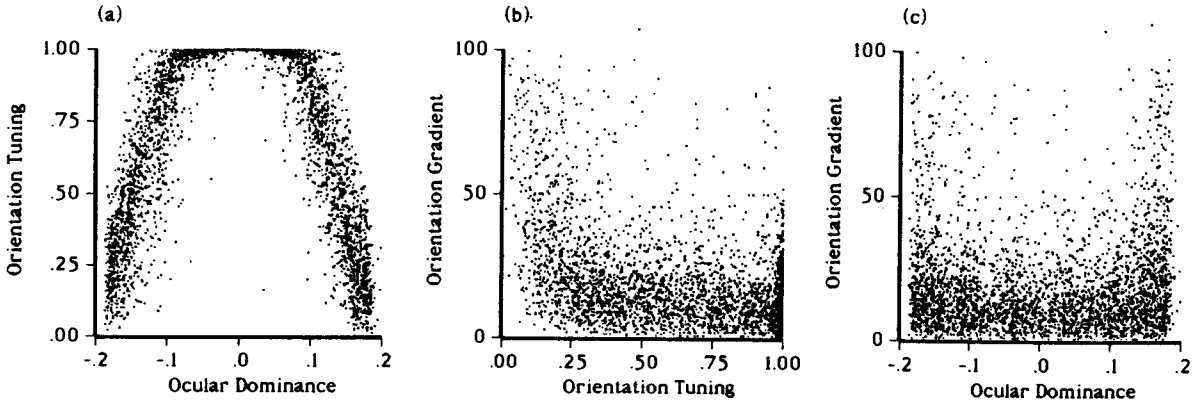

Fig. 9a–c. Scatter plots for a simulation with the same parameter values as the one illustrated in Fig. 4, showing the distributions of each of the three pairs of values of $|z|$ (orientation tuning), $n * w_n$ (ocular dominance) and grad(θ) (orientation gradient), obtained after 410 program steps. Gradient values in (**b**) and (**c**) are degrees per array unit (3.7). Each point represents the values present at a single array location

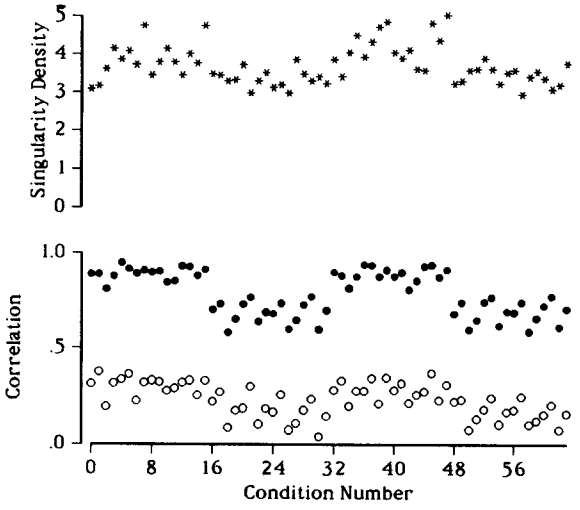

Fig. 10. The effect of variations in the parameters $k_z, k_n, \bar{w}_z, \bar{w}_n, \sigma_z, \sigma_n$ on three different measures of the model's output. A subset of points in this parameter space is mapped onto the horizontal axis of the figure in the following way: each parameter takes on one of two values $k_z, k_n \in (1.5, 6)$; $\bar{w}_z, \bar{w}_n \in (-12, 1)$; $\sigma_z, \sigma_n \in (0.02, 0.08)$ thereby defining a 6-bit binary value, the order of bits corresponding to the order of parameters. The bit is 1 for the higher value of the parameter and 0 for the lower value. For example if $(k_z, k_n, \bar{w}_z, \bar{w}_n, \sigma_z, \sigma_n) = (1.5, -12, 1, 0.2, 0.02)$ the horizontal axis value $= 010110 = 22$. A simulation was run for each of the 64 possible parameter combinations; other parameters had the values given in Fig. 4. The vertical axes show singularity density (upper panel) and (lower panel) the correlation between $|z|$ and $|n * w_n|$ (filled circles) and the correlation between grad(θ) and $|n * w_n|$ (open circles) measured for a single simulation run with each of the parameter combinations. The effect of a given parameter can be identified by a corresponding periodicity (or lack of one) in the graph. For example the absence of any changes with periods of 4, 8 or 32 on the x axis indicate the lack of effect of parameters $\bar{w}_n$, $\bar{w}_z$, and k_z respectively

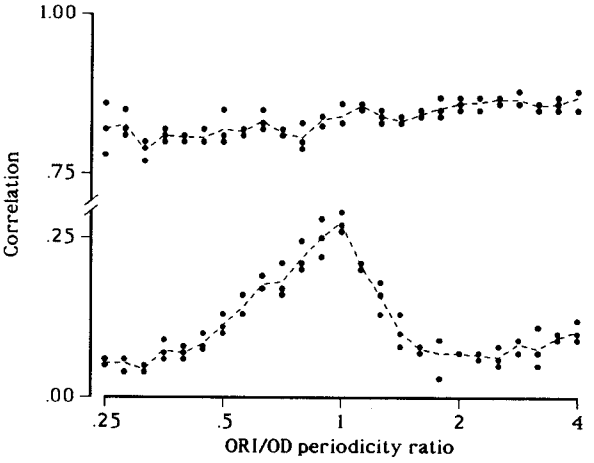

Fig. 11. The coupling between ocular dominance and orientation gradient, as a function of the relative periodicities of the two sets of columns. Periodicities were varied keeping the geometric mean of the two constant; when the ratio $= 1$, each had a period $= 12$ array units; for ratios of 0.25 and 4 the periods were 6 : 24, and 24 : 6 respectively. Each point on the graph is a calculation based on the outcome of a single simulation, and the dashed lines connect the mean for each of three simulations at each periodicity ratio. The upper set of points shows the correlation between ocular dominance, $|n * w_n|$, and orientation modulus $|z|$, which is relatively unaffected by periodicity ratio. The lower set of points shows the correlation between $|n * w_n|$ and orientation gradient, grad(θ), which is highest at a periodicity ratio of one. This result also emphasises the independence of the two measures of coupling between columns

icity ratio between orientation and ocular dominance columns: the correlation is largest when the columns have the same periodicity. This may be because the regions of highest orientation gradient have a spacing that is about half the period of the orientation domains. Coupling will be greatest when these regions tend naturally to be spaced as far apart as the centers of the ocular dominance columns. Note that the correlation between $|z|$ and $|n * w_n|$ shown in the same figure remains high and relatively constant at all frequency ratios, emphasizing the independence of this measure and the correlation between grad(θ) and $|n * w_n|$.

Finally, the degree of elongation (or spatial anisotropy) of the orientation domains has effects on the degree of coupling: if the domains are anisotropic i.e. elongated in one consistent direction, then the regions of high orientation gradient become reduced in extent, as does the number of singularities. This has the effect of reducing the measured correlation.

5 Discussion

5.1 Parameters

The two lateral interaction functions (w_n and w_z) used to generate the ocular dominance and orientation maps are defined by 5 parameter values each (λ, $\bar{w}$, g, k and β); four more parameters are used to define the initial conditions of n and z (means and standard deviations at $t = 0$), and parameter a defines the strength of the interaction between n and z during development. This gives a total of 15 parameters, and it is commonly supposed that any model with more than 5 degrees of freedom can explain almost anything. In fact, most of the parameter values used here are either constrained, within reasonable limits, by the data, or else have relatively small effects on the outcome of the model. For example, λ_n, λ_z, g_n, g_z, β_n, β_z and a are chosen, as described above, to fit data values that are known well (e.g. λ_n, λ_z, β_n and β_z), or approximately (e.g. the growth rates g_n and g_z). a is chosen to give patterns that reproduce the measured relations between singularities and the orientation gradient map, and ocular dominance stripes. As demonstrated above (Fig. 10), values of k_z, k_n, $\bar{w}_z$, $\bar{w}_n$, σ_z and σ_n are uncritical over a range of values of each (e.g. $[-12 \leqslant \bar{w}_z, \bar{w}_n \leqslant 1]$; $[1.5 \leqslant k_z, k_n \leqslant 6]$; $[0.02 \leqslant \sigma_z, \sigma_n \leqslant 0.08]$) although certain combinations lead to too high a density of singularities, or to very low correlations between the ocular dominance and gradient maps.

5.2 Fractures

A novel feature of the paper by Blasdel and Salama (1986) was the use of a gradient operator to characterise the orientation map, and to investigate its relation to the layout of ocular dominance stripes. The gradient map in the monkey was shown to be periodic, with regions of high gradient forming a series of ridges encircling regions of low gradient. Regions of highest gradient, termed 'fractures' were found to be closely associated with the cytochrome oxidase blobs, and with the centers of ocular dominance columns.

It is likely that orientation patterns of the kind found in the monkey necessarily contain periodic variations in orientation gradient. If the patterns are characterised by 180° singularities, these will tend to have an average spacing about half that of the iso-orientation domains (Swindale 1982). Since the orientation gradient must be high (strictly speaking it is infinite) in a singularity, periodicity in the gradient map may partly reflect the spacing of the singularities. Another reason is that the result of differentiating a function that is periodic (e.g. a sine wave) and then taking the magnitude (as is done to calculate the orientation gradient) will generally be a function that has twice the period of the original. The existence of periodic variations in orientation gradient is not a priori dependent on the coupling with ocular dominance, since orientation patterns generated in the absence of coupling contain periodic variations in gradient. A different algorithm (Durbin and Mitchison 1990) which produces an orientation map resembling that found in the monkey, independently of any interaction with ocular dominance, also produces a periodic map of orientation gradient.

Figure 4b illustrates the fact that the orientation gradient map produced by the model is spatially continuous. The distribution of gradient values (e.g. Fig. 9b or c) is also continuous. Because of this it seems inappropriate to refer to regions of highest gradient as 'fractures' (e.g. the line segments displayed in Fig. 4c), since a fracture implies a discontinuous change in gradient. There was no evidence that the model produces truly discontinuous orientation changes anywhere other than in the singularities. This same caveat possibly applies to the monkey, since Fig. 1b suggests that the real orientation gradient map is also continuous. This possibility is reinforced by the observation that the magnitudes of orientation gradient values are similar in both the model and the monkey data. The black regions in Fig. 1b for example correspond to a gradient value of 45°/40 μm and a display of regions of similar gradient in the model produced a similar pattern of spots or short strips which mostly coincide with the singularities. The threshold for display of the line segments in Fig. 4c was equivalent to a gradient of ≈25°/40 μm, which is probably similar to the threshold used by Blasdel and Salama for their Fig. 1c. Against this, it could be argued that the cortex is not a continuous substrate, and that since adjacent neurons can be separated by distances of about 40 μm, a jump in orientation preference of 25° or more in 40 μm is to all intents and purposes a discontinuity.

5.3 Cytochrome oxidase patches

Many of the features of the pattern of cytochrome oxidase staining found in the monkey (Horton and Hubel 1981; Horton 1984) are reproduced by the model (Fig. 4d). As in the monkey, patchy regions of poor orientation selectivity (i.e. low values of $|z|$) are centered in the ocular dominance stripes and thereby aligned into rows. Patches in neighbouring rows are often aligned and connected by thin bridges crossing the borders between ocular dominance columns, a feature also observed in the monkey (Horton 1984; Tootell et al. 1988). Regions of high orientation gradient often run along these bridges (Fig. 4d). It is not clear at present why the model produces such alignments, but they are a consistent feature of the results.

Overall however, the distribution of 'CO spots' produced by the model seems somewhat less regular than is actually observed, and this is especially manifest in the rather irregular spacing of the model patches along the ocular dominance stripes. Another observation which makes it difficult to draw a simplistic analogy between $|z|$ and cytochrome oxidase activity is that the cytochrome patches are present before birth in the monkey, probably appearing at the same time that ocular dominance columns begin to form (Horton 1984). Very little structure in the model's map of orientation selectivity (i.e. $|z|$) is present at this stage. Cytochrome oxidase however is no more than an indicator

of metabolic activity (Wong–Riley et al. 1978; Wong–Riley 1979), and it might be naïve to suppose that its distribution will always match that of orientation selectivity, especially in fetal tissue. Horton (Fig. 48, 1984) made the additional observation that in the monocular region of striate cortex, where ocular dominance stripes are absent, the cytochrome patches are about twice as large and widely spaced as in the immediately adjacent binocular region. This suggests that the cytochrome system has an intrinsic low periodicity of its own which is overridden by the ocular dominance system in binocular cortex. This may be the case of the large spacing of the patches along the ocular dominance stripes, and the tendency of neighbouring patches to join up.

5.4 Relation between orientation gradient, orientation selectivity, singularities and ocular dominance

An unanticipated result of the simulations was the reproduction of the relation between the orientation gradient map and the ocular dominance map, with ridges of high gradient showing a tendency to run either parallel or orthogonal to the stripes. As in the monkey, this seems only to be a general tendency, and the ridges can be found intersecting stripe borders at a variety of angles (Fig. 6). Statistically (i.e. Fig. 9c) the relationship is weak even though visual inspection of the patterns gives a strong impression of a relation. The relationship seems to be a secondary consequence of a close association between regions of high orientation gradient, and regions where $|z|$ is low. As noted in the previous section, the latter regions tend to be connected or elongated either along the direction of a stripe, or orthogonally to neighbouring regions in an adjacent stripe, and the gradient ridges tend to follow these directions.

5.5 Reasons for the inter-dependence of the two columnar systems

This paper has explored the consequences of the idea that the rate of emergence of orientation selectivity is slowest in the centers of emerging ocular dominance stripes. There seems little reason to doubt that this is true, at least in the upper cortical layers, since it is well established that regions in which orientation selectivity is poor or absent coincide with the centers of ocular dominance stripes (Livingstone and Hubel 1984). It is not known however, how this correlation emerges during development; nor is it known whether the link is directly causal, or the result of an independent developmental process that affects both systems. For example, a framework of cytochrome spots might be set up early on that guided the development of both orientation and ocular dominance columns. This could then be the common cause of the structural relationship between the two systems. If this does not happen, it seems more likely that the process of formation of orientation columns would be guided by the segregation of ocular dominance columns than vice versa, since the latter process occurs at an earlier stage in the visual pathway than orientation, and is therefore less likely to be influenced by the development of connections responsible for the emergence of orientation selectivity at later stages in the pathway.

Assuming that this is the case, the dependence has been modelled here by supposing that $\partial z/\partial t$ is proportional to a term $(1-|n * w_n|)^a$ (3.5). The justification for this formulation is that it seems to work. It would be desirable however to derive this, or some similar relationship from a more detailed analysis of the ways in which orientation columns and ocular dominance columns might interact during development. Two possible approaches to doing this will be suggested here. The first derives from a general consideration of factors determining stability in developing systems. Underlying much theoretical work on development, as well as on the behaviour of neural nets, is the idea that systems progress from initially unstable, disordered states, to stable ordered ones, in which certain measures of the system are either maximized (e.g. the correlation between pre- and post-synaptic firing) or minimized (e.g. an energy function) (Linsker 1986). These measures are generally averages and usually some parts of the system can be considered more stable than others. In the present case, regions of high stability are the centers of ocular dominance columns (which thereby resist perturbations such as monocular deprivation), and regions where $|z|$ is large early in development i.e. regions where $|z * w_z|$ is large. It is possible that some more global measures of stability will be further optimised if it can be arranged that stable regions of one system overlap with less stable regions of another, that is, if $|z * w_z|$ is negatively correlated with $|n * w_n|$ as happens here.

A second, related, possibility is that there is a factor that exerts overriding control over synaptic plasticity at the level of individual cells, or cells in the same column. This does not mean that different parts of the cell might not be modified in different ways during development, but that if and when plasticity was turned off this affected the whole cell (or column of cells) and not parts of it. According to this notion, the overall degree of synaptic plasticity present in the cortex could vary from cell to cell, and would vary depending on a cell's developmental history, and there it was located in relation to the surrounding columnar structures. Thus cells in the center of an ocular dominance stripe might achieve a configuration of inputs that conferred stable ocular dominance values early in development (i.e. a configuration producing a high correlation between pre- and post-synaptic activity). By stabilising their inputs early on, these cells would lose their ability to change or acquire other response properties which require synaptic modification, such as orientation preference or the sharpness of orientation tuning. This would lead to an interaction similar to that modelled here, and is thus a possible cause of the observed structural links between ocular dominance and orientation columns.

5.6 Tangential variation in plasticity

It is well established that plasticity in the visual cortex is not a single-valued entity that changes over time

(giving rise to a single critical period for the whole visual cortex) but is a quantity that may vary depending on the cortical layer involved (Blakemore et al. 1978; LeVay et al. 1980) or on response property (Berman and Daw 1977). The hypothesis studied here implies that at certain intermediate periods of development, plasticity may also vary with tangential position in the cortex i.e. from column to column. A consequence of this is that the distribution of molecules involved in regulating plasticity may exhibit a patchy distribution that would be manifest only at intermediate stages of development. Transient patchiness in the distribution of the 1c subtype of the 5HT receptor has recently been observed in kittens between the ages of 30–60 days (Dyck and Cynader 1990), which raises the possibility (but no more) that this receptor subtype plays a role in modulating plasticity in the cat in a manner similar to that discussed here. It is not known whether this same phenomenon occurs in the monkey, but it clearly will be fruitful to look for signs of transient patchiness in the expression of this and other significant molecules in the visual cortices of both cats and monkeys.

5.7 Consequences of the inter-dependence of the two columnar systems

There may be functional consequences of the arrangement of columns demonstrated by Blasdel and Salama and modelled here. As originally suggested by Hubel and Wiesel (1974b) one of the factors that has probably influenced the evolution of striate cortex is the need for all possible combinations of eye and orientation preference to be present in a region of cortex defined as the 'point image', that is the region containing cells responsive to a single location in visual space. An even allocation (referred to elsewhere as 'coverage', Cynader et al. 1987) of orientation preferences to each eye would presumably be a requirement in order to be able to see equally well through either eye. As demonstrated by Hubel and Wiesel (1974b) the cortical point image is comparable in size to only a few complete sets of orientation or ocular dominance 'hyper-columns' and thus the geometrical constraints on obtaining uniform coverage are likely to be significant. Maximising the variation of orientation preference within the centers of ocular dominance stripes, by ensuring that regions of rapid orientation change fall within the centers, might therefore be a way of ensuring a more uniform allocation of orientations to every retinal location in each eye. Whether or not this is the case remains uncertain, however, an advantage of having morphologically realistic models of ocular dominance and orientation columns is that the possible role of these geometrical constraints can be investigated computationally. The following paper (Swindale 1991) is therefore devoted to a consideration of the ways in which columnar structure may constrain the achievement of uniform coverage.

Acknowledgements. This work was supported by grants from the MRC of Canada (MA 9211) from the British Columbia Health Care Research Foundation, and IRIS of Canada. I thank Graeme Mitchison his comments.

References

Barlow HB, Pettigrew JD (1971) Lack of specificity of neurones in the visual cortex of young kittens. J Physiol London 218:98P–100P

Batschelet E (1981) Circular statistics in biology, Academic Press, New York

Berman N, Daw NW (1977) Comparison of the critical periods for monocular and directional deprivation in cats. J Physiol 265:249–259

Blakemore C, Garey LJ, Vital-Durand F (1978) The physiological effects of monocular deprivation and their reversal in the monkey's visual cortex. J Physiol Lond 283:223–262

Blasdel GG, Salama G (1986) Voltage-sensitive dyes reveal a modular organization in monkey straite cortex. Nature 321:579–585

Bonhoeffer T, Grinvald A (1990) Novel aspects of the functional architecture of area 18 in cat visual cortex. Soc Neurosci (abstr) 16:292

Cynader MS, Swindale NV, Matsubara JA (1987) Functional topography in cat area 18. J Neurosci 7:1401–1413

Durbin R, Mitchison G (1990) A dimension reduction framework for understanding cortical maps. Nature 343:644–647

Dyck R, Cynader M (1990) Serotonin receptors exhibit a transient columnar and laminar distribution in developing cat visual cortex. Soc Neurosci (abstr) 16:987

Hendrickson AE, Hunt SP, Wu J-Y (1981) Immunocytochemical localization of glutamic acid decarboxylase in monkey striate cortex. Nature 292:605–607

Horton JC (1984) Cytochrome oxidase patches: a new cytoarchitectonic feature of monkey visual cortex. Phil Trans R Soc Lond B 304:199–253

Horton JC, Hubel DH (1981) Regular patchy distribution of cytochrome oxidase staining in primary visual cortex of macaque monkey. Nature 292:762–764

Hubel DH, Livingstone MS (1981) Regions of poor orientation tuning coincide with patches of cytochrome oxidase staining in monkey striate cortex. Soc Neurosci (abstr) 7:357

Hubel DH, Wiesel TN (1963) Receptive fields of cells in striate cortex of very young, visually inexperienced kittens. J Neurophysiol 26:994–1002

Hubel DH, Wiesel TN (1968) Receptive fields and functional architecture of monkey striate cortex. J Physiol (Lond) 195:215–243

Hubel DH, Wiesel TN (1972) Laminar and columnar distribution of geniculo-cortical fibers in the macaque monkey. J Comp Neurol 146:421–450

Hubel DH, Wiesel TN (1974a) Sequence regularity and geometry of orientation columns in the monkey striate cortex. J Comp Neurol 158:267–294

Hubel DH, Wiesel TN (1974b) Uniformity of monkey striate cortex: a parallel relationship between field size, scatter, and magnification factor. J Comp Neurol 158:295–306

Hubel DH, Wiesel TN, LeVay S (1977) Plasticity of ocular dominance columns in monkey striate cortex. Phil Trans R Soc Lond B 278:131–163

Hubel DH, Wiesel TN, Stryker MP (1978) Anatomical demonstration of orientation columns in macaque monkey. J Comp Neurol 177:361–380

LeVay S, Hubel DH, Wiesel TN (1975) The pattern of ocular dominance columns in macaque striate cortex revealed by a reduced silver stain. J Comp Neurol 159:559–576

LeVay S, Stryker MP, Shatz CJ (1978) Ocular dominance columns and their development in layer IV of the cat's visual cortex: a quantitative study. J Comp Neurol 179:223–244

LeVay S, Wiesel TN, Hubel DH (1980) The development of ocular dominance columns in normal and visually deprived monkeys. J Comp Neurol 191:1–51

Linsker R (1986) From basic principles to neural architecture: emergence of orientation columns. Proc Natl Acad Sci USA 83:8779–8783

Livingstone MS, Hubel DH (1984) Anatomy and physiology of a color system in the primate visual cortex. J Neurosci 4:309–356

Rakic P (1977) Prenatal development of the visual system in the rhesus monkey. Phil Trans R Soc Lond B 278:245–260

Sherk H, Stryker MP (1976) Quantitative study of orientation selectivity in visually inexperienced kittens. J Neurophysiol 39:63–70

Swindale NV (1980) A model for the formation of ocular dominance stripes. Proc R Soc Lond B 208:243–264
Swindale NV (1981) Patches in monkey visual cortex. Nature 293:509–510
Swindale NV (1982) A model for the formation of orientation columns. Proc R Soc Lond B 215:211–230
Swindale NV, Matsubara JA, Cynader MS (1987) Surface organization of orientation and direction selectivity in cat area 18. J Neurosci 7:1414–1427
Swindale NV (1991) Coverage and the design of striate cortex. Biol Cybern (this volume)
Tootell RBH, Hamilton SL, Silverman MS, Switkes E (1988) Functional anatomy of macaque striate cortex. I Ocular dominance, binocular interactions, and baseline conditions. J Neurosci 8:1500–1530
Wiesel TN, Hubel DH (1974) Ordered arrangement of orientation columns in monkeys lacking visual experience. J Comp Neurol 158:307–318
Wiesel TN, Hubel DH, Lam DMK (1974) Autoradiographic demonstration of ocular-dominance columns in the monkey striate cortex by means of transneuronal transport. Brain Res 79:273–279
Wong-Riley MTT, Merzenich MM, Leake PA (1978) Changes in endogenous enzymatic reactivity to DAB induced by neuronal inactivity. Brain Res 141:185–192
Wong-Riley MTT (1979) Changes in the visual system of monocularly sutured or enucleated kittens demonstrable with cytochrome oxidase histochemistry. Brain Res 171:11–28

Dr. N. V. Swindale
Dept. of Ophthalmology
University of British Columbia
2550 Willow Street
Vancouver, BC
Canada V5Z 3N9